

Application of Commercial Non-Dispersive Infrared Spectroscopy Sensors for Sub-ambient Carbon Dioxide Detection

Michael J. Swickrath* and Molly Anderson[†]
NASA Johnson Space Center, Houston, TX, 77058

Summer McMillin[‡]
Engineering and Science Contract Group - Jacobs Technology, Houston, TX, 77058

Craig Broerman[§]
Engineering and Science Contract Group - Hamilton Sundstrand, Houston, TX, 77058

Monitoring carbon dioxide (CO₂) concentration within a spacecraft or spacesuit is critically important to ensuring the safety of the crew. Carbon dioxide uniquely absorbs light at wavelengths of 3.95 micrometers (μm) and 4.26 μm . As a result, non-dispersive infrared (NDIR) spectroscopy can be employed as a reliable and inexpensive method for the quantification of CO₂ within the atmosphere. A multitude of commercial off-the-shelf (COTS) NDIR sensors exist for CO₂ quantification. The COTS sensors provide reasonable accuracy as long as the measurements are attained under conditions close to the calibration conditions of the sensor (typically 21.1°C (70.0°F) and 1 atmosphere). However, as pressure deviates from atmospheric to the pressures associated with a spacecraft (8.0–10.2 pounds per square inch absolute (psia)) or spacesuit (4.1–8.0 psia), the error in the measurement grows increasingly large. In addition to pressure and temperature dependencies, the infrared transmissivity through a volume of gas also depends on the composition of the gas. As the composition is not known *a priori*, accurate sub-ambient detection must rely on iterative sensor compensation techniques.

This manuscript describes the development of recursive compensation algorithms for sub-ambient detection of CO₂ with COTS NDIR sensors. In addition, the source of the exponential loss in accuracy is developed theoretically. The basis of the loss can be explained through thermal, Doppler, and Lorentz broadening effects that arise as a result of the temperature, pressure, and composition of the gas mixture under analysis. This manuscript provides an approach to employing COTS sensors at sub-ambient conditions and may also lend insight into designing future NDIR sensors for aerospace application.

*Analyst, Crew and Thermal Systems Division, 2101 NASA Parkway, EC211, Houston, TX, 77058, AIAA Member.

[†]Analysis Lead, Crew and Thermal Systems Division, 2101 NASA Parkway, EC211, Houston, TX, 77058, AIAA Member.

[‡]Project Engineer, EVA and Health Systems Group, 2224 Bay Area Blvd., Houston, TX, Member AIAA.

[§]Project Engineer, CxP and Advanced Systems Group, 2224 Bay Area Blvd., Houston, TX, Member AIAA.

Nomenclature

CO ₂	= Carbon dioxide
COTS	= Commercial off-the-shelf
CRDS	= Cavity ring-down spectroscopy
ECLSS	= Environmental control and life support
EVA	= Extra-vehicular activity
H ₂ O	= Water
IR	= infrared
ISS	= International Space Station
N ₂	= Nitrogen
NDIR	= Non-dispersive infrared
O ₂	= Oxygen
ppm	= Parts per million
psia	= Pounds per square inch
VSA	= Vacuum swing adsorption

I. Introduction

CARBON dioxide produced through respiration can accumulate rapidly within closed spaces. If not managed, the crew's respiratory rate increases, headaches and hyperventilation occur, vision and hearing are affected, and cognitive abilities decrease. Consequently, development continues on a number of CO₂ removal technologies for human spacecraft and spacesuits. Terrestrially, technology development requires precise performance characterization to qualify promising air revitalization equipment. On-orbit, instrumentation is required to identify and eliminate unsafe conditions. This necessitates accurate *in situ* CO₂ detection.

A variety of techniques exist to quantify CO₂ in the atmosphere. One low-cost yet sensitive technique is non-dispersive infrared (NDIR) spectroscopy. Infrared absorption is associated with vibrational and rotational energy transitions of covalent bonds that are susceptible to energetic perturbations at a particular wavelength.¹⁻⁴ A bond stretching mode exists at 4.26 micrometers (μm) for CO₂. Excitation leads to rotational energy transitions producing a multitude of distinct absorption lines. As a result, the Beer-Lambert law can be used to correlate an intensity change to gas concentration, $A' = 1 - \exp(-k_\nu L)$, where A' is the absorbed fraction of the light ($A' = A/A_0$ where A_0 represents gas absorbance when the sample is devoid of the species of interest), L is the optical path length, and k_ν is the absorption coefficient. A number of commercial off-the-shelf (COTS) NDIR sensors are readily available for CO₂ detection.

However, the accuracy of COTS sensors are highly application specific. Absorption lines undergo broadening through a variety of mechanisms that diminish the sensitivity and precision of these sensors.⁵ First, spectral lines have a contribution to width which arises from the Heisenberg uncertainty principle as it applies to spectroscopic measurements. Specifically, excited states have a finite lifetime governed by a decay process such that absorption measurements produce ensemble-averaged results. Second, random collisions perturb the energy levels of the components of a gas sample. This is referred to as 'pressure-broadening' and is strongly influenced by system pressure where high pressure increases the likelihood of molecular interaction. Pressure broadening is also composition dependent since kinetic excitation is influenced by the momenta of the molecules involved in an excitation event. Lastly, thermal energy imparts random Doppler velocities to each molecule which serves to 'blur' a line over a spectral range. This indicates that detection is also influenced by system temperature.

A number of pressures, under consideration for space exploration, are summarized in detail elsewhere.⁶ The International Space Station (ISS) and Space Shuttle were designed for 14.7 pounds per square inch (psia), and the Shuttle can also operate at a pressure of 10.2 psia. For extra-vehicular activity (EVA), pressures of 4.3 psia are under consideration while the spacesuit must operate at 8.0 psia to interface with vehicles and as high as 23.1 psia under contingency operations such as decompression sickness mode. Moreover, atmospheric composition is dictated by the Environmental Control and Life Support System (ECLSS) and can range from low to high relative humidity with several orders of magnitude higher CO₂ partial pressure than exist on Earth. Technology development necessitates hardware testing over a wide variety of pressures,

temperatures, and compositions. COTS-NDIR sensors are attractive from a testing stand-point as they are low cost and resolute; however, detection over a wide range of pressures, temperatures, and gas compositions poses a challenge to employing these sensors. This manuscript establishes one approach to the temperature/pressure/composition compensation of COTS-NDIR sensors. Furthermore, theoretical techniques to generate mixed gas spectra as a function of temperature and pressure are developed for potential application in aerospace sensor design.

II. Scaling Heuristics

COTS-NDIR sensors provide an inexpensive and flexible means to quantify CO₂ concentration in a gas sample. These sensors rely on the approximation that absorption measurements under one set of conditions (*i.e.* test conditions) can be corrected through scaling based on another set of conditions (*i.e.* calibration conditions). This method is referred to as the non-overlapping line approximation⁷ and it tends to produce reasonable results as long as the pressure and temperature of a system does not deviate significantly from calibration conditions.

$$\frac{A}{P} = f\left(\frac{u}{P}\right) \quad (1)$$

In Eq. (1), A represents the total absolute absorption, P is the total pressure, and u is the absorber amount ($u = \rho_i L$) which depends on the component density of the gas sample, ρ_i ($\rho_i = y_i P / RT$ assuming ideality where y_i is the component mole fraction). The parameter L is the path length of the optics of the sensor. Consequently, the molar fraction of a component can be quantified via Eq. (2) through inversion of function f .

$$y_i = \frac{RT}{L} f^{-1}\left(\frac{A}{P}\right) \quad (2)$$

Using the non-overlapping line approximation, scaling is accomplished presuming $y_i \rho_i = y_{i,o} \rho_{i,o}$ so that compensation is accomplished according to the following relationship where the function g is the inverse of f .

$$y_i = y_{i,o} \frac{T}{T_o} g\left(\frac{P_o}{P}\right) \quad (3)$$

In Eq. (3), $y_{i,o}$ is the mole fraction reported by the sensor and P_o and T_o are the sensor calibration pressure and temperature. The mole fraction is proportional to absorbance which is also proportional to the voltage output of a sensor. These proportionalities are all implicitly captured within the coefficients of function g . Literature exists suggesting g can take the form of a polynomial.^{1,2} Alternatively, in this work, g has been represented as a power-law expression. This approach is physically more representative of the physics captured by the Beer-Lambert law. It will be shown within this manuscript that the power law produces reasonable agreement with experimental data.

As previously mentioned, not all gases have the same capacity to cause pressure broadening. This renders NDIR detection composition dependent. The composition dependency is generally accounted for through the notion of ‘equivalent pressure’, P_e . The equivalent pressure modifies the reported value for composition specific spectral broadening effects.^{1,2} Coefficients ϕ_i represent the broadening of spectral lines relative to nitrogen (*i.e.* $\phi_{N_2} = 1$).

$$P_e = P \left[1 + \sum_j^{\text{Components}} (\phi_j - 1) y_j \right] \quad (4)$$

P_e is substituted for P in Eq. (3). The typical major constituents of the gas-phase in space exploration include CO₂, H₂O, N₂, and O₂. However, the sensor compensation routines developed within this investigation were established based on test data in an oxygen-free environment. As a result, Eq. (5) represents the compensation function established in this work for carbon dioxide detection with COTS-NDIR sensors.

$$y_{CO_2} = y_{CO_2,o} \frac{T}{T_o} \left[\alpha \left(\frac{P_o}{P} \frac{1}{[1 + (\phi_{H_2O} - 1) y_{H_2O} + (\phi_{CO_2} - 1) y_{CO_2}]} \right)^\beta \right] \quad (5)$$

In Eq. (5), α and β are power-law coefficients accounting for pressure-broadening, $\phi_{\text{H}_2\text{O}}$ is the foreign-gas broadening coefficient associated with water-vapor, and ϕ_{CO_2} is the self-broadening coefficient for CO_2 .

Expression (5) provides a closed-form analytical expression for off-calibration compensation of COTS-NDIR sensors providing the four compensation parameters can be determined. However, the complication arises that the actual carbon dioxide concentration depends on a function directly dependent on the carbon dioxide concentration. Consequently, expression (5) must be solved iteratively. This was achieved through a Newton-Raphson scheme in which an objective function, F , was defined along with a corresponding derivative with respect to carbon dioxide fraction $F' = dF/dy_{\text{CO}_2}$.

$$F = y_{\text{CO}_2} - \alpha y_{\text{CO}_2,0} \frac{T}{T_0} \left[\frac{P}{P_0} (1 + (\phi_{\text{H}_2\text{O}} - 1)y_{\text{H}_2\text{O}} + (\phi_{\text{CO}_2} - 1)y_{\text{CO}_2}) \right]^{-\beta} \quad (6)$$

$$F' = \alpha\beta y_{\text{CO}_2,0} \frac{T}{T_0} \left[\frac{P}{P_0} (\phi_{\text{CO}_2} - 1) \right] \left[\frac{P}{P_0} (1 + (\phi_{\text{H}_2\text{O}} - 1)y_{\text{H}_2\text{O}} + (\phi_{\text{CO}_2} - 1)y_{\text{CO}_2}) \right]^{(-\beta-1)} \quad (7)$$

The Newton-Raphson method is a relatively efficient recursive technique seeking roots of a real-valued function with a property of quadratic convergence. Employing expressions (6) and (7), the Newton-Raphson scheme proceeds from iteration n to $n + 1$ as follows.

$$y_{\text{CO}_2}^{n+1} = y_{\text{CO}_2}^n - \frac{F}{F'} \quad (8)$$

After each iteration, a convergence check is performed $\tau = |y_{\text{CO}_2}^{n+1} - y_{\text{CO}_2}^n|$. When the successive error between iterations τ , is below a pre-defined threshold, convergence is presumed. The actual fraction of CO_2 for the first iteration was set to the reported fraction of CO_2 per the non-compensated sensor reading to initialize the routine, $y_{\text{CO}_2}^0 = y_{\text{CO}_2,0}$. The tolerance was set to 1×10^{-8} and convergence was generally achieved within three to four iterations. Situations where convergence required significantly more than three to four iterations did arise and were indicative of instrumentation errors (*e.g.* sensor-drift requiring a re-zero and re-span procedure). Consequently, counting iteration during the recursive scheme provided an additional measure to identify and eliminate sensor anomalies real-time during testing. The iterative technique described above provided the methodology to correct COTS-NDIR sensors across a wide variety of temperatures, pressures, and compositions. As a result, this enabled the application of these sensors across a wide variety experiments performed at the NASA Johnson Space Center (JSC).

III. Experimental Characterization

The first step in verifying the iterative technique involved building a custom sensor test stand. A multitude of COTS-NDIR sensors were evaluated during this investigation from two primary vendors. Vaisala HUMICAP[®] HMT-334 relative humidity sensors and CARBOCAP[®] GMT-221/222 CO_2 sensors (Vaisala, Vantaa, Finland) were employed for the initial investigation. Subsequent investigations relied on the Li-Cor 840A Gas Analyzers (Li-Cor Environmental, Lincoln, NE). Sensors were ranged from 0% to 1% up to 0% to 5% CO_2 with respect to standard temperature and pressure.

A custom test apparatus was built for the preliminary investigation to characterize sensor performance at a reduced pressure environment. The initial test stand was capable of regulating pressure and introducing precise quantities of a dry pre-mixed CO_2/N_2 gas source. A chamber with laboratory air was initially de-pressurized to near vacuum and then refilled with dry N_2 for a number of times to remove all potentially NDIR sensitive gas species. After the last evacuation procedure, the chamber was then refilled with the pre-mixed gas source to a desired pressure ranging from 2–15 psia. Once the pressure was achieved, the mass flow controllers were powered off and sensor measurements were collected for several minutes. Following this procedure, the mass flow controllers were actuated again until the next desired pressure was reached. This process was followed up until ambient pressure was achieved. A Rosemount Analytical XStream HASXEE-IM-HS gas analyzer (Emerson Process Management, Pittsburgh, PA) was used to provide actual gas concentrations.

These preliminary experiments provided a basis for the calibration function f . However, without the capability to introduce precise amounts of water vapor, complete compensation could not be achieved on this test-stand alone.

Subsequent investigations relied on a pre-existing test stand established to collect performance data for amine swing beds being tested at the JSC.^{8,9} This test stand was capable of precise CO₂ and water vapor introduction through a Bronkhorst Controlled-evaporator and mixing unit (Bronkhorst, Bethlehem, PA). The loop was de-pressurized for sub-ambient testing as low as 3.8 psia (pounds per square inch, absolute) using a Varian TriScroll™ 300 vacuum pump (Varian, Inc., Agilent Technologies, Santa Clara, CA). Gas flow within the loop was controlled using a Micronel® U51DX-024KK-5 fan (Micronel® AG, Tagelswangen, Switzerland) which was subsequently measured by a Teledyne Hastings HFM-200 flow meter. The test article allowed for the collection of transient data over a range of relative humidity and CO₂ partial pressures. A cavity ring-down mass spectroscopy (CRDS) unit (Picarro, Sunnyvale, CA) was plumbed into the loop in series with the CO₂ sensors. CRDS takes multiple light intensity readings as it travels between opposing optical mirrors over the course of micro-seconds. The intensity decays as the light traverses the optical path over several measurements providing data with which to establish precise species concentrations. The cavity within the CRDS is maintained at a constant pressure of 140 millimeters of mercury (mm Hg) and 10 °C (50 °F) irrespective of the pressure and temperature of the test stand. Consequently, the CRDS unit was considered as the actual reading providing data with which to find the appropriate constants in expression (5). Whereas the CRDS collects measurements over a wide temperature/pressure environment in which we place high confidence, the cost and size of the CRDS unit relative to COTS-NDIR sensors renders it prohibitive for wide-scale application.

IV. Verification of the Compensation Method

As previously mentioned, a custom test stand was built to explore the relationship between pressure and carbon dioxide concentration on reported readings for the COTS-NDIR sensors. Success in these efforts would significantly widen the opportunities for application of these sensors. CARBOCAP® GMT-221/222 CO₂ sensors were analyzed in this phase of the investigation. The test team employed several sensors which were ranged from 0% to 1%, 0% to 3%, and 0% to 5%. Pre-mixed gas samples were introduced to an evacuated bell jar over pre-defined pressure increments. The test stand involved a bell jar, vacuum pump, and a series of mass flow controllers connected to pre-mixed dry gas sources, along with temperature and pressure sensors for data collection.

Figure 1 demonstrates typical results obtained in this analysis for a 0–1% CARBOCAP® GMT-222 sensor. The left panel shows the raw data collected in the investigation. The dashed line indicates the actual composition within the bell jar of known volume which originally starts at a given pressure and temperature. As the pressure in the jar is increased using the pre-mixed gas, the actual concentration within the jar asymptotically approaches the concentration of the gas source. As indicated in the left panel of Fig. 1, the reported readings deviate significantly from the actual values at low pressures. As pressure increases to 1 atmosphere standard (atm), the compensated values and the reported readings begin to converge.

At the time of this investigation, it became obvious compensation was necessary; however, the exact compensation relationship was not known. As a result, three potential compensation functions were considered: (1) compensation employing a scalar α_k to determine the degree of non-linearity associated with pressure compensation, (2) pressure compensation via a power-law, and (3) pressure/composition compensation via a power law using an equivalent pressure described by Eq. (4). The right panel of Fig. 1 demonstrates the results considering the three compensation functions. First, for all k measurements (on the order of 10,000), unique α_k values were determined demonstrating how significantly the reported reading needed re-scaled to collapse upon the actual concentration. All fitting was performed using a objective function and a Nelder-Mead downhill simplex method.¹⁰ Once these values were determined, the natural logarithm of α_k was plotted against the logarithm of pressure in atmospheres. The near linear relationship between the logarithms of α_k and pressure seem to suggest a power law relationship is a reasonable approximation. Secondly, the power law compensation functions were defined along with the compensation parameters α , β , ϕ_{CO_2} . The values of the fitting parameters were once again determined using the simplex method and the relationships were plotted in both panels of Fig. 1.

The results of this exercise are demonstrated in two particularly salient features in Fig. 1. First, for accurate compensation, it is clear that knowledge of both pressure and composition are necessary. Second, the power law relationship between pressure and reported reading means that as the pressure is decreased, measurement noise is dramatically amplified through the compensation algorithm. The latter observation suggests that COTS-NDIR sensors will have a practical limit in reduced pressure detection where the noise

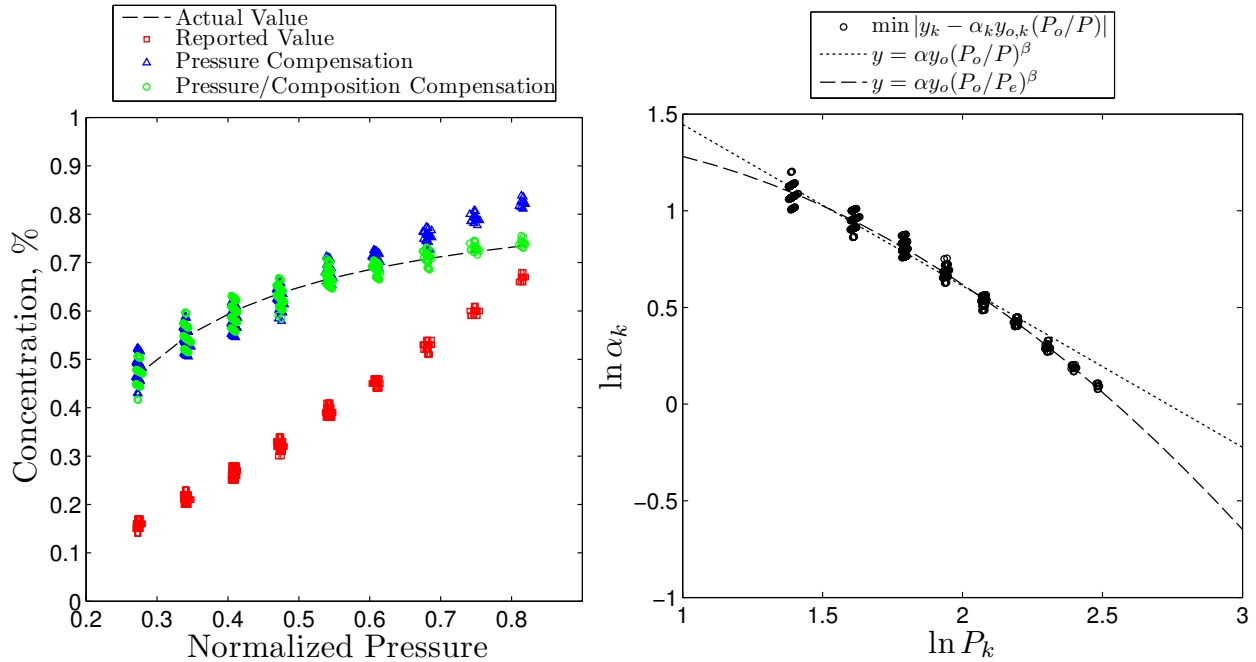


Figure 1: Compensation of reduced pressure Vaisala CARBOCAP[®] GMT-221 readings for an evacuated bell jar re-pressurized with 0.87% CO₂ with balance of N₂. The left panel shows sensor reported values, sensor values compensated according to pressure, and sensor values compensated according broadening effects captured by the equivalent pressure. The right panel demonstrates a unique scalar value α_k , required to compensate each individual reading along with how pressure and pressure/composition compensation relate to these readings.

introduced through compensation renders the sensors inaccurate for application. The Vaisala sensors revealed that this appears to be somewhere around 0.6–0.7 atm although it depends largely on the desired application of the sensor and what level of error is acceptable for test purposes. The manufacturer guarantees pressure compensation results in an error of 1.5% of the full-scale range plus 2% of the reading as long as the system pressure is between 70–130 kilopascal (kPa) (0.7–1.3 atm) for this particular sensor.

Results collected within this investigation demonstrated two important relationships. Sensor reported readings deviated significantly from actual concentration at reduced pressure and gas–broadening effects are significant. Since spacecraft and spacesuits are designed to provide humidity in the range of 25–75%,¹¹ the latter observation indicates that accurate compensation routines cannot be developed without accounting for broadening effects introduced by water vapor. Moreover, pressure relevant to spacesuit application are as low as 4.1 psia (0.28 atm).⁶ Consequently, the next phase of the investigation sought to characterize and develop compensation routines for sensors capable of detection of CO₂ and H₂O at lower pressures. Therefore the Li-Cor 840A[®] gas analyzer was employed for this analysis that advertises a pressure compensation range of 0.15–1.13 atm. However, during operation, the built-in pressure compensation was only found to be accurate when measurements deviated by approximately 0.1 atm from calibration pressure. The manufacturer later suggested that the supplied compensation routine should only be used at reduced pressures after re-zeroing and re-spanning the instrument at the pressure of interest. Since optimal pressures for spacecraft and spacesuits is still a matter of debate, and since EVA pre-breathe protocol requires dynamic pressure acclimation with constant CO₂ detection, it was necessary to develop in-house compensation techniques that span the entire range of pressure anticipated for space exploration.

Controlled introduction of CO₂ and water vapor was facilitated by an existing test stand described in detail elsewhere.^{8,9} The test stand included a moisture and carbon dioxide removal swing–bed which was actuated to maintain an environment safe for space exploration as defined elsewhere.¹¹ A cavity ring–down mass spectroscopy (CRDS) unit provided what was considered the actual readings as discussed in a preceding

section. Figure 2 demonstrates the results collected during this investigation. Performance was assessed at four individual pressures as demonstrated by the top graph. Data were collected at the outlet side of the swing-bed for several cycles and then switched to the inlet of the swing-bed for several more cycles at each pressure. The 840A gas analyzer recorded the detection cell pressure, temperature, and reported CO_2 and H_2O concentrations, thereby providing all necessary data for the compensation routine.

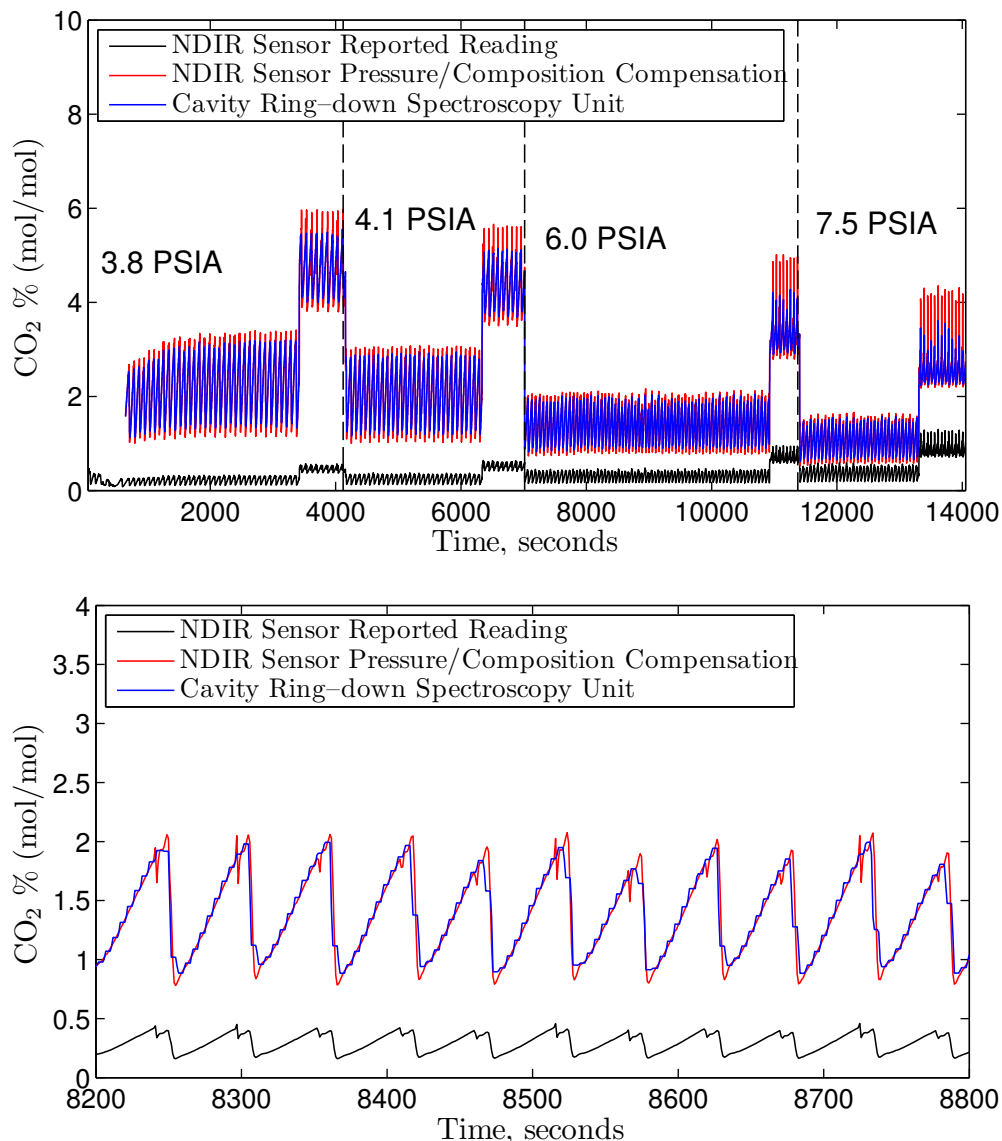


Figure 2: Compensation of reduced pressure Li-Cor 840A[®] readings within the swing-bed performance characterization test loop as compared to the Picarro CRDS unit over a variety $\text{CO}_2/\text{H}_2\text{O}$ concentrations and pressures. The top panel shows sensor reported values and sensor values compensated according broadening effects over multiple pressures. The bottom panel shows sensor reported values and sensor values compensated according broadening effects at the scale of individual cycles at 6.0 psia.

As indicated in the top graph of Fig. 2, the reported reading differs substantially from readings collected by the CRDS unit before compensation. Moreover, the error appears more prominent at lower pressures which agrees with previous observations with other NDIR sensors. Utilizing the data collected by the 840A and CRDS gas analyzers, the parameters α , β , ϕ_{CO_2} , and $\phi_{\text{H}_2\text{O}}$, of Eq. (5) were fit for the 840A sensor via the simplex method employed in previous phases of the investigation. As evidenced in the top graph,

the fitted parameters resulted in good agreement with the CRDS unit. The bottom graph illustrates the compensated results at 6.0 psia (0.41 atm) with increased resolution at the cyclic-scale. At the resolution of cycles, agreement appears reasonable between the CRDS and 840A. The CRDS results demonstrate a ‘stair-stepped’ trend which is associated with the fact that the CRDS reports to the data acquisition system at a frequency of 1 Hz while the measurements are actually obtained over the course of 1.6–2.2 seconds. Furthermore, at the peak of each profile, an anomalous decrease in CO₂ concentration is observed. This artifact was introduced by the test loop which requires pneumatic actuation of the swing-bed valve when cycling to a fresh bed. During the actuation process, a small amount of gas was introduced into the test loop resulting in a short perturbation in system pressure. Whereas the CRDS has a means to control its detection cell pressure, the 840A does not have this capability. Consequently, in the compensation procedure, the pressure perturbation results in an amplification of this perturbation. In spite of these artifacts, the agreement between the NDIR and CRDS appears suitable. The compensated NDIR sensor results were used to perform a material balance on the test loop demonstrating the swing-bed removal rate and the CO₂ and H₂O injection rates were in agreement.

In summary, NDIR is an attractive method for CO₂ quantification since the technology is affordable and the instrumentation involved is flexible with quick installation and connection to data acquisition systems. However, these results in aggregate demonstrate that pressure and molecular broadening can drastically alter the reported readings of COTS-NDIR sensors when used for reduced pressure CO₂ detection. As demonstrated, these effects can be quantified and corrected. Through corrections, we were able to demonstrate that accurate data could be collected. This is promising for test applicability; however, the development of these sensors were subject to requirements that were very different than constraints imposed during space exploration. The latter phase of this investigation sought to develop a first principles competency in NDIR physics in the hopes that the knowledge could be applied in aerospace sensor design.

V. Molecular Spectra Calculations

Since NDIR sensors are inexpensive and flexible, it is desirable to develop methods to numerically compensate these sensors for off-nominal application. The preceding results indicate this is possible for some commercially available NDIR sensors which is encouraging for the terrestrial qualification of developing hardware. However, for application in spacecraft and spacesuits, it is not always practical to employ COTS-NDIR sensors. First, the sensors were not necessarily designed for these types of applications and, therefore, might result in noise amplification as conditions dynamically change within a closed volume. Second, the communication protocols from instrumentation to the core flight software of the caution and warning system might not be optimized. Third, the packaging of the instrumentation and processing equipment was developed without consideration for deployment in a spacecraft and spacesuit, thereby creating problems during interfacing commercial counterparts with existing systems. Therefore, it is attractive to have a first principles understanding of how pressure, temperature, and molecular species concentrations influence infrared spectra. The following section outlines the prediction of spectral signatures that arise as a result of kinetic theory.

Two approaches exist for predicting infrared (IR) spectra: (1) *ab initio* molecular dynamics calculations can be employed to determine the energy states and resulting IR spectra of an ensemble of molecules,^{12–14} and (2) spectral line parameters can be obtained from ‘line list’ databases such as HITRAN¹⁵ to build spectra *line-by-line*. The former approach requires the molecular ensemble to be large for accurate predictions which involves a high computational cost. The latter approach can provide accuracy with limited computational resources. The detailed derivation for this analysis is documented thoroughly elsewhere⁵ and will be explained briefly below.

A. Beer-Lambert Law

As previously discussed, absorbance at wavelength ν through pathlength L is quantified according to the Beer-Lambert law, $A = A_o [1 - \exp(-k_\nu L)]$. This relationship depends on the absorption coefficient, k_ν . The absorption coefficient can be written as follows for a sample that behaves as an ideal gas.

$$k_\nu = \frac{qP}{k_B T} \sigma_\nu \quad (9)$$

In Eq. (9), q is the volume mixing ratio (unitless), k_B is the Boltzmann constant (1.380658×10^{-23} J/K), and σ_ν is the molecular cross-section (cm^2). The product of the component spectral line intensity S ($\text{cm}^{-1}/(\text{molecule}/\text{cm}^2)$) and spectral line shape at wavenumber ν , g_ν ($1/\text{cm}^{-1}$), result in the molecular cross-section, $\sigma_\nu = Sg_\nu$. Furthermore, noting transmissivity at ν is the complement of absorption $\tau_\nu = 1 - A'_\nu$ (unitless), the following more convenient expression for the Beer-Lambert law is formulated.

$$\tau_\nu = \exp \left[\frac{-qPL}{k_B T} Sg_\nu \right] \quad (10)$$

Equation (10) indicates that the absorption coefficient can be calculated for each wavelength pending the spectral line intensity and the line shape are known.

B. Line Shape

Line shape g_ν , is subject to a number of broadening mechanisms and is particularly sensitive to mixture composition and pressure. This section presumes the spectrum of a single gas in the mixture is of interest so that subscripts and superscripts can be neglected in the development of terms contributing to line shape and intensity. Subsequent sections will discuss how the species spectra are combined for the mixture transmittance spectrum. The line centers ν_c (cm^{-1}), tend to increase linearly with pressure from a zero-center position ν_c° (cm^{-1}), according to the air-broadened pressure-shift coefficient δ , *viz.*

$$\nu_c = \nu_c^\circ + \delta \frac{P}{P_\circ} \quad (11)$$

Parameters ν_c° and δ are readily obtained for common atmospheric gases from the HITRAN database.

While line centers is influenced linearly by pressure as captured by the pressure-shift coefficient, Doppler broadening arising from thermal motion blurs the line shape in a Gaussian manner providing a half-width γ_D .

$$\gamma_D = \nu_c \left[\frac{2k_B T}{m_j c^2} \right]^{1/2} \quad (12)$$

In expression (12), m_j is the molecular mass of component j (kg), and c is the speed of light (cm/s). In near-zero pressures, Doppler broadening dominates the line shape term.

An additional species-dependent pressure-broadening effect is captured by the Lorentz line shape which becomes more prominent as pressure increases. In particular, collisions between similar and dissimilar particles result in different energy transitions. The Lorentz line width can be described by the following relationship.

$$\gamma_L = [(1 - q)\gamma_{L_a}^\circ + q\gamma_{L_s}^\circ] \left(\frac{P}{P_\circ} \right) \left(\frac{T_\circ}{T} \right)^n \quad (13)$$

In equation (13), $\gamma_{L_a}^\circ$ is the air-broadened half-width contribution, $\gamma_{L_s}^\circ$ is the self-broadened half-width contribution, and n is the coefficient of temperature dependence of air-broadened half-width. These three parameters can be obtained in the HITRAN database.

The Doppler and Lorentz broadening contributions are combined yielding the Voigt profile, f_v .

$$f_v = \frac{1}{\pi^{3/2}} \frac{\gamma_L}{\gamma_D^2} \int_{-\infty}^{+\infty} \frac{\exp(-t^2)}{(\gamma_L/\gamma_D)^2 + [(\nu - \nu_c)/\gamma_D - t]^2} dt \quad (14)$$

The function representing the Voigt profile is non-analytic. Thus a numerical technique is warranted to generate an approximate answer. This can be achieved through Gaussian quadrature although the infinite bounds must be handled carefully (*e.g.* a transformation of variables can be used to modify the boundaries). However, the form of expression (14) lends itself to much more straightforward integration through Gauss-Hermite quadrature due to the numerator term which was employed in this investigation. After calculating the Voigt profile, one subsequent adjustment is made for far-wing effects.

$$g_\nu = \frac{\nu}{\nu_c} \frac{\tanh(hc\nu/2k_B T)}{\tanh(hc\nu_c/2k_B T)} f_v \quad (15)$$

In Eq. (15), h is Planck's constant (6.62618×10^{-34} m²·kg/s). It should be noted that caveats exist for special cases in which line-coupling and speed-dependent broadening produce important contributions. However, for most typical spectral calculations, the Voigt profile is considered a reasonable approximation and was therefore employed in this analysis.

C. Line Intensity

The line intensity, S , is the remaining calculation required to generate spectra for gas mixtures. The line intensity at off-nominal (*i.e.* off-calibration) conditions requires accounting for the thermal influence on the rotational and vibrational partition functions, Q_r and Q_v .

$$S(T, P) = S_o \frac{Q_r(T_o) Q_v(T_o)}{Q_r(T) Q_v(T)} \frac{\exp(hcE_o/k_B T)}{\exp(hcE_o/k_B T_o)} \left[\frac{1 - \exp(-hc\nu_c/k_B T)}{1 - \exp(-hc\nu_c/k_B T_o)} \right] \quad (16)$$

In the expression above, E_o is the lower state energy provided by the HITRAN database. Expression (16) can be solved from a tabulation of total internal partition sums parameterized as a function of temperature.¹⁶

From this point, equations (10) through (16) provide the expressions required to generate a spectrum pending line and intensity parameters are known. The line and intensity parameters have been meticulously documented within the HITRAN database at 296 K providing all the data required to predict transmissivity spectra for components typically found within the atmosphere of Earth. Figure 3 illustrates the results of this process. In the calculations, wavenumber was discretized in increments of 0.25 cm⁻¹, which was parametrically found to be a suitable value as further discretization significantly increased computational time while it did not result in a different value for the integrated area under the absorptivity curve ($A' = 1 - \tau_\nu$).

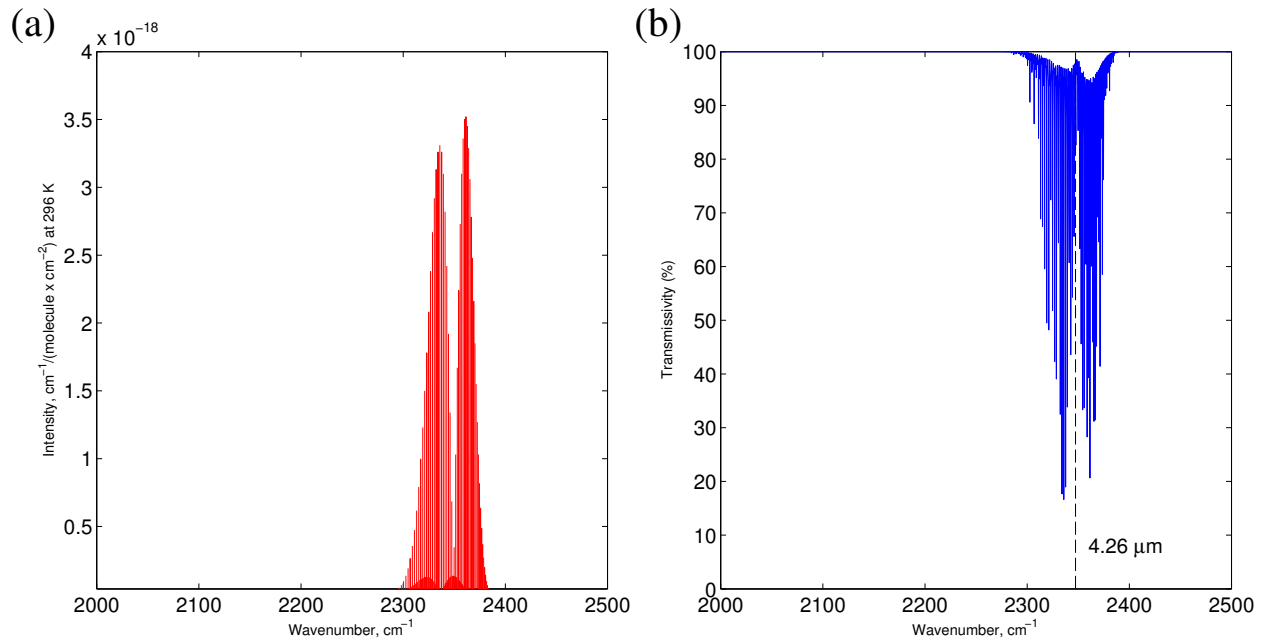


Figure 3: Molecular spectrum for CO₂ at 370 parts per million (ppm) in air. The left panel demonstrates the intensity of a transition in energy states over a range of wavenumber. The right panel demonstrates the transmissivity spectrum obtained based on intensity, broadening, and energy state data obtained from the HITRAN database.¹⁵

Figure 3(a) illustrates the line positions and intensities for carbon dioxide at 296 K. This chart shows strong spectral activity in the wavenumber range of 2300-2400 cm⁻¹. As a consequent, the Vaisala CARBOCAP[®] line is designed to detect in this range using a light source with a wavelength of 4.26 μm. The Li-Cor 840A provides a broad-band IR source with filters in front to provide light at 4.26 and 3.95 μm.

The expected IR spectrum arising from the Voigt profile calculations for 370 ppm of CO₂ in an atmosphere of 1 atm at 296 K is demonstrated in Fig. 3(b). The concentration of 370 ppm was chosen since it falls within the range of observed atmospheric CO₂ concentrations and it was the design point of the Li-Cor 840A sensor. An optical pathlength of 14 cm was used for the calculation which is associated with the path length of the 840A gas analyzer. It is evident in Fig. 3(b) that at a wavelength of 4.26 μm, the transmissivity is still greater than 95% for this low concentration but that it is still less than 100% indicating detection would be possible for a path length of 14 cm. This analysis suggests sensor design is constrained by expected CO₂ concentration in the applied environment. Specifically, for aerospace application, the pressure, temperature, and expected CO₂ concentration range could be set and a parametric investigation could be performed on L to determine the optimal path length for the desired accuracy and resolution. It is possible that over a wide range of conditions, a sensor array may be required along with logic to determine which sensors from the array should be referenced under the measurement conditions.

D. Transmittance Spectrum of the Gas Mixture

Preceding sections discuss in detail the expected line shape and intensity contributions for an individual gas j over all spectral lines denoted by i . During an IR spectroscopy measurement of gas mixture, the observed profile is a coalescence of individual contributions. The prediction of the observed transmittance profile is generated from a product of the contributing gas spectra.

$$\tau_\nu = \prod_j \prod_i \tau_{\nu_{i,j}} = \exp \left[-\frac{PL}{k_B T} \sum_j q_j \sum_i \sigma_{\nu_{i,j}} \right] \quad (17)$$

Eq. (17) was employed for a variety of gases at different compositions in air at 1 atm and 296 K in an effort to verify these calculations. These results are displayed in figure 4.

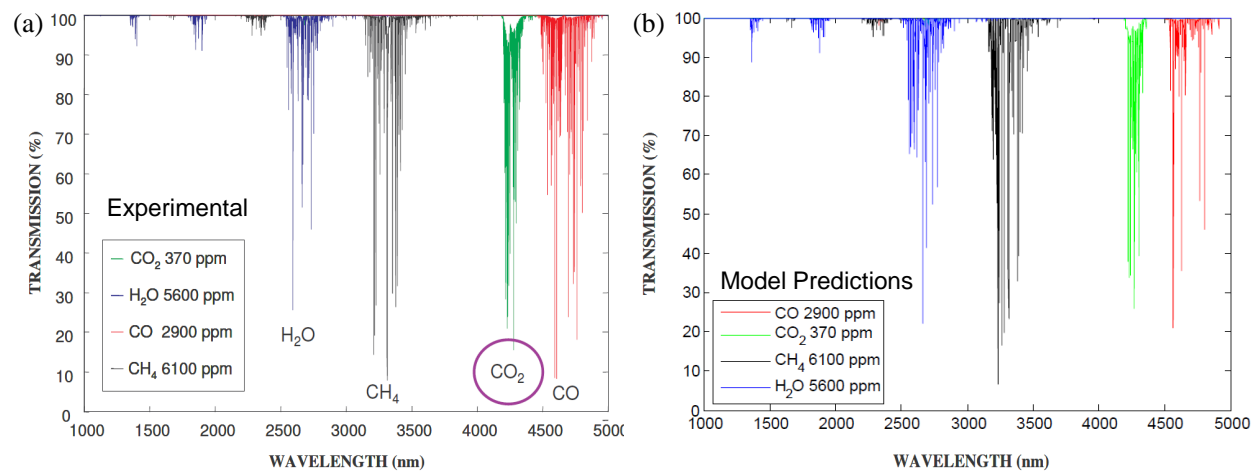


Figure 4: Comparison of experimentally determined spectra (left) and numerical predictions (right) for a mixed gas sample. Experimental results were obtained from a Vaisala product brochure for the CARBOCAP[®] sensor series.¹⁷

As indicated in Fig. 4, the location of IR active regions for the components agree well between the spectral predictions and experimentally collected results from Vaisala.¹⁷ Transmissivity predictions show comparable agreement as well, although a path length of 14 cm was assumed since data with respect to the experimental instrument were not available. This analysis suggests the spectral calculations produce reasonably accurate results and may serve as an analysis tool for sensor design for aerospace application. Consequently, it was of interest to confirm source of the power law relationship discussed in previous sections through a more fundamental analysis. These results are demonstrated in figure 5.

Furthermore, to explore the relationship between transmissivity and total system pressure, carbon dioxide concentration was fixed at 370 ppm while the system pressure was varied from 0.05 atm to 1.00 atm in

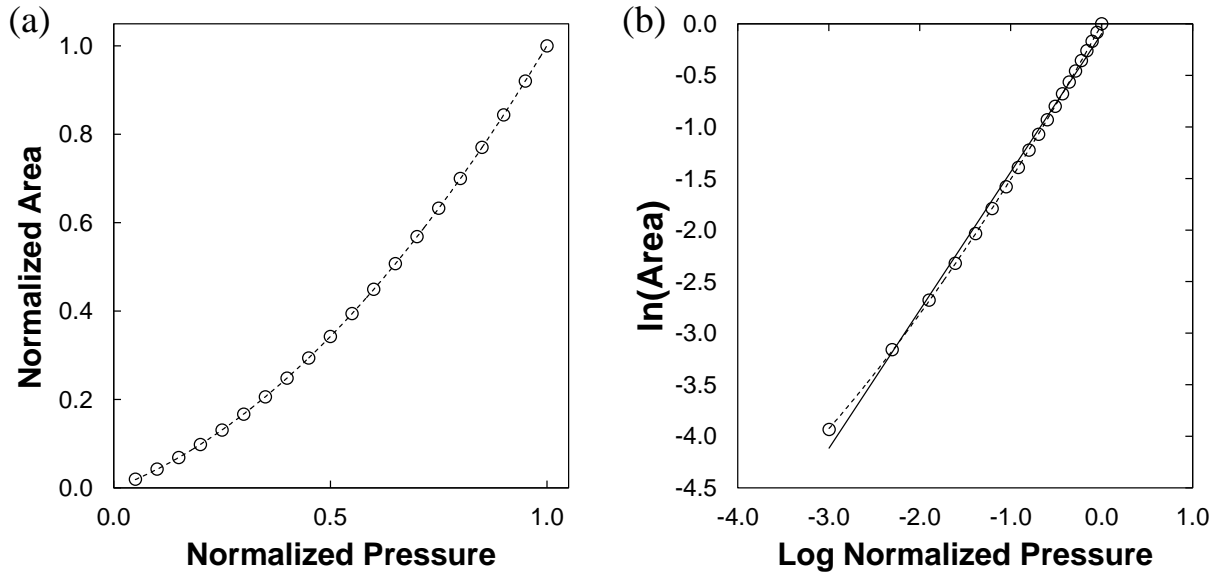


Figure 5: Numerical results demonstrating a loss of absorptivity as the partial pressure of air is decreased with constant CO₂ concentration (370 ppm). (a) The integrated area under the absorption spectrum normalized by the area at 1.0 atm and 296 K. (b) log-log plot of area and pressure relationship with a black-line demonstrating a linear fit which corresponds to compensation without accounting for composition.

increments of 0.05 atm. Rather than compare the transmissivity predictions at 4.26 μm , the integrated area under the absorptivity curve was instead used as a surrogate in this calculation. This was chosen since it provides the pressure dependency across the entire IR active region of the spectrum of CO₂. The calculated area was small and was subsequently normalized by the area at 1.00 atm to better demonstrate the trend. As shown by Fig. 5(a), the area varies non-linearly with pressure and ostensibly follows a power law relationship. The log-log plot in Fig. 5(b) shows that there is slight deviation from the power law relationship (solid black line) with pressure which supports the experimental observations displayed in Fig. 1 that component broadening effects are important for accurate reduced pressure CO₂ detection. Consequently, the spectral calculation routine seems to reproduce experimental observations and could plausibly be employed to tailor sensors for aerospace applications.

VI. Conclusions

Desired spacecraft and spacesuit pressure are still under consideration. As a result, efforts toward hardware development generally require performance characterization at a variety of pressures. COTS-NDIR sensors are attractive due to their flexibility and affordability for CO₂ detection. However, results demonstrated herein show a precipitous loss of accuracy at even modest deviations from off-calibration conditions which provides the impetus to develop a better understanding on NDIR theory.

As indicated in this work, heuristic scaling arguments were utilized to develop reasonable compensation techniques. Experimental results confirmed this approach and provided evidence composition broadening significantly alters spectra when pressure is reduced. Consequently, a recursive compensation technique was developed with the Newton-Raphson method which was subsequently verified through experimentation.

In an effort to better understand sensor compensation, as well as to lend insight into the design of custom CO₂ NDIR sensors, spectral line shape calculations were performed. The spectral calculations were verified with experimental results collected from literature. Moreover, the results confirm a loss of accuracy in reduced pressure application. The analysis seems to also provide support for the power law correction and the importance of accounting for composition broadening during compensation. Future work may include using the spectral calculation code for the parametric analysis across a variety of compositions, temperatures, and pressures, in the development of reduced pressure NDIR sensors or sensor arrays.

VII. Acknowledgements

The authors gratefully acknowledge Matt Vogel of the Engineering and Science Contract Group (Houston, TX) for many great discussions regarding the principles of NDIR. Furthermore, the authors thank the Space Suit & Crew Survival Systems Branch for providing analytical and experimental resources for this investigation.

Mathematical Annotation

A. Variables

A	= Absorbance, [unitless]
A'	= Relative absorbance, [unitless]
E_o	= Lowest energy state, [J]
F	= Objective function, [unitless]
F'	= Derivative of objective function, [unitless]
f_ν	= Voigt profile at ν , [$1/\text{cm}^{-1}$]
g_ν	= Spectral luine shape at ν , [$1/\text{cm}^{-1}$]
k_ν	= Absorption coefficient, [m^{-1}]
L	= Optical length path, [cm]
m	= Molecular mass, [kg/kmole]
n	= Iteration number, [No.]
P	= Pressure, [atm -or- psia]
q	= Volume mixing ratio, [unitless]
Q_r	= Rotational partition function, [unitless]
Q_v	= Vibrational partition function, [unitless]
S	= Spectral line intensity, [$\text{cm}^{-1}/(\text{molecule}/\text{cm}^2)$]
T	= Temperature, [K]
y	= Mole fraction, [unitless]

B. Greek Letters

α	= Compensation parameter, [unitless]
β	= Compensation parameter, [unitless]
δ	= Air-broadened pressure coefficient, [unitless]
γ_D	= Doppler-broadened half-width, [cm^{-1}]
γ_L	= Lorentz-broadened half-width, [cm^{-1}]
γ_{L_a}	= Air-broadened contribution to Lorentz half-width, [cm^{-1}]
γ_{L_s}	= Self-broadened contribution to Lorentz half-width, [cm^{-1}]
ν	= Wavenumber, [cm^{-1}]
ν_c	= Wavenumber line center, [cm^{-1}]
ν_c^o	= Wavenumber line center at reference conditions, [cm^{-1}]
ϕ	= Broadening coefficient, [unitless]
σ_ν	= Molecular cross-section, [m^2]
τ	= Convergence tolerance, [unitless]
τ_ν	= Transmissivity at ν , [unitless]

C. Sub/super-scripts

- = Associated with reference conditions
- ν = Associated with a given wavenumber
- i = Denotes a particular species
- j = Denotes a particular species

D. Physical Constants

- c = Speed of light, [2.997925×10^8 m/s]
- h = Planck's constant, [6.626180×10^{-34} J-s]
- k_B = Boltzmanns constant, [1.380658×10^{-23} J/K]
- P_o = Reference pressure, [1 atm –or– 14.696 psia]
- R = Universal gas constant, [8.314472 J/mol-K]
- T_o = Reference pressure, [296.15 K]

References

- ¹McDermitt, D., Welles, J., and Eckles, R., "Effects of temperature, pressure and water vapor on gas phase infrared absorption by CO₂," *LI-COR Inc*, 1993.
- ²Welles, J. and McDermitt, D., "Measuring carbon dioxide in the atmosphere," *Agronomy*, Vol. 47, 2005, pp. 287.
- ³Burch, D., Singleton, E., and Williams, D., "Absorption line broadening in the infrared," *Applied Optics*, Vol. 1, No. 3, 1962, pp. 359–363.
- ⁴Burch, D., Gryvnak, D., Patty, R., and Bartky, C., "Absorption of Infrared Radiant Energy by CO₂ and H₂O. IV. Shapes of Collision-Broadened CO₂ Lines," *Journal of the Optical Society of America*, Vol. 59, No. 3, 1969, pp. 267–280.
- ⁵Gordley, L., Marshall, B., and Allen Chu, D., "LINEPAK: Algorithms for modeling spectral transmittance and radiance," *Journal of Quantitative Spectroscopy and Radiative Transfer*, Vol. 52, No. 5, 1994, pp. 563–580.
- ⁶Campbell, P. and Henninger, D., "Recommendations for Exploration Spacecraft Internal Atmospheres: The Final Report of the NASA Exploration Atmospheres Working Group," *JSC-63309*, January 2006.
- ⁷Holter, M., Nudelman, S., Suits, G., Wolfe, W., and Zissis, G., *Fundamentals of infrared technology*, Macmillan New York, 1962.
- ⁸Swickrath, M., Anderson, M., McMillin, S., and Broerman, C., "Simulation and Analysis of Vacuum Swing Adsorption Units for Spacesuit Carbon Dioxide and Humidity Control," *Proceedings of the International Conference on Environmental Systems*, American Institute of Astro. & Aero., Portland, OR, 2011, AIAA-2011-5243.
- ⁹McMillin, S., Broerman, C., Swickrath, M., and Anderson, M., "Testing and Results of Vacuum Swing Adsorption Units for Spacesuit Carbon Dioxide and Humidity Control," *Proceedings of the International Conference on Environmental Systems*, American Institute of Astro. & Aero., Portland, OR, 2011, AIAA-2011-5244.
- ¹⁰Nelder, J. and Mead, R., "A simplex method for function minimization," *The computer journal*, Vol. 7, No. 4, 1965, pp. 308.
- ¹¹NASA, "Recommendations for Exploration Spacecraft Internal Atmospheres: The Final Report of the NASA Exploration Atmospheres Working Group," *CxP-70024 Rev. C.*, January 2006.
- ¹²Rappe, A. and Goddard III, W., "Charge equilibration for molecular dynamics simulations," *The Journal of Physical Chemistry*, Vol. 95, No. 8, 1991, pp. 3358–3363.
- ¹³van Gunsteren, W. and Berendsen, H., "Computer simulation of molecular dynamics: Methodology, applications, and perspectives in chemistry," *Angewandte Chemie International Edition in English*, Vol. 29, No. 9, 1990, pp. 992–1023.
- ¹⁴Amos, R., Handy, N., Knowles, P., Rice, J., and Stone, A., "AB-initio prediction of properties of CO₂, NH₃, and CO₂ ··· NH₃," *The Journal of Physical Chemistry*, Vol. 89, No. 11, 1985, pp. 2186–2192.
- ¹⁵Rothman, L., Rinsland, C., Goldman, A., Massie, S., Edwards, D., Flaud, J., Perrin, A., Camy-Peyret, C., Dana, V., Mandin, J., et al., "The HITRAN molecular spectroscopic database and HAWKS (HITRAN Atmospheric Workstation): 1996 edition," *Journal of Quantitative Spectroscopy and Radiative Transfer*, Vol. 60, No. 5, 1998, pp. 665–710.
- ¹⁶Fischer, J., Gamache, R., Goldman, A., Rothman, L., and Perrin, A., "Total internal partition sums for molecular species in the 2000 edition of the HITRAN database," *Journal of Quantitative Spectroscopy and Radiative Transfer*, Vol. 82, No. 1, 2003, pp. 401–412.
- ¹⁷Vaisala, "Vaisala CARBOCAP® Carbon Dioxide Sensors: What is CO₂?" Tech. rep., Vaisala Inc.